

Evaluation of CFD as a Surrogate for Wind-Tunnel Testing: Experimental Uncertainty Quantification for the UPWT Flow Survey Test

Erin P. Hubbard*
Jacobs, Cleveland, OH 44135, USA

Heather P. Houlden†
ViGYAN, Inc., Hampton, VA 23666, USA

A series of wind tunnel tests are being performed at the Unitary Plan Wind Tunnel (UPWT) at NASA Langley Research Center to assess the validity of using computational fluid dynamics (CFD) as a surrogate for wind tunnel testing. In order to make proper comparisons, uncertainties in CFD results and experimental data must be well understood. The material presented highlights the methods, assumptions, and inputs used to achieve experimental uncertainty estimates. Results for a small subset of tunnel conditions and variables of interest from the first test in the series, the Flow Survey Test, are highlighted and sample CFD comparisons are shown. The bulk of the results from this work are used for comparisons in other AIAA conference papers related to this test series.

I. Nomenclature

d_2	=	Range statistic correction factor
MC	=	Local Mach number
PTC	=	Flow survey rake pitot pressure (psia)
QC	=	Local dynamic pressure (psfa)
R	=	Prefix signifying range normalized by d_2
\tilde{R}	=	Median range
UL	=	Upper Limit
$UPWT$	=	Unitary Plan Wind Tunnel
$XRAKE, X$	=	Axial location of rake probe tip (inches)
$YRAKE, Y$	=	Lateral location of rake probe tip (inches)
$ZRAKE, Z$	=	Vertical location of rake probe tip (inches)

II. Introduction

In any experiment, understanding the magnitude of uncertainty in values of interest is critical to drawing meaningful conclusions or confirming the efficacy of the study. When the study itself revolves around comparison of computationally driven vs. experimental results, the understanding of uncertainty in the quantities being compared becomes even more vital. This paper focuses on the experimental uncertainty quantification aspect of a wind tunnel test performed in the UPWT. The first in a series of several experiments using different model types and configurations, this Flow Survey Test is reminiscent of a tunnel characterization and calibration test that gathers test-section characteristics such as boundary layer profile/thickness and free-stream flow variables (i.e. pressure, temperature, Reynolds number, velocity, flow uniformity, and flow angularity) at various stations and tunnel conditions. Not only does this data serve as an initial comparator to “empty tunnel” CFD, it also provides data that can be used as boundary conditions in subsequent CFD simulations. The distinct approaches to determining random and systematic uncertainty estimates are presented, both of which are relevant aspects of uncertainty when comparing experimental results to CFD. Results for a small subset of

*Data Engineer, AIAA Member.

†Senior Research Engineer, 30 Research Dr., AIAA Senior Member.

tunnel conditions and variables of interest are highlighted as examples of what this analysis provides.

III. Description of Flow Survey Experiment

The Langley UPWT is a closed-circuit continuous flow supersonic pressure tunnel. The flow survey test acquired data throughout the UPWT's 4-foot by 4-foot by 7-foot long test section measuring pressures, temperatures, dew point, and boundary layer profiles at 48 distinct tunnel conditions. A detailed description of this facility is presented in Reference [1]. Tunnel conditions are defined by different combinations of set points for Mach number (from Mach 2.3 to 4.6), Reynolds number (from 1 to 5 million/ft), total temperature (125 to 150°F) and total pressure (700 to 11000 psfa). A flow survey rake and boundary layer rakes were used to gather flow field data. The flow survey rake spanning the height of the test section was mounted to an articulating sting, and boundary layer rakes were mounted to the test section side walls. Facility pressure and temperature are measured in the settling chamber and serve as a reference for many test section conditions. Several other measurements such as wall pressures, rake body pressures, and angles were used to identify facility status and model attitude. Facility and model measurements were used to calculate local free stream conditions such as Mach number, Reynolds number, dynamic pressure, and flow angularity.

A. Model Descriptions

The flow survey rake shown in Figure 1 consisted of a vertical array of nineteen 20° half-angle cone-tipped five-hole probes spaced two inches apart. Probe number 1 was located at the top of the rake, and probe 19 was at the bottom of the rake. The top and bottom rake probes were 18 inches above and below the tunnel centerline, respectively. This resulted in the top and bottom probe being positioned six inches from the test section ceiling and floor. Static pressure probes offset on the survey rake were collocated with probes 1, 5, 11, 15, and 19. Five-hole probes in the array were replaced by double-shielded thermocouple probes to perform the temperature survey. The rake was mounted to an articulating sting capable of traversing the rake axially from the front to the rear of the test section and laterally across the test section width. This provided cross-sectional measurements of the flow at different stations along the length of the test section.

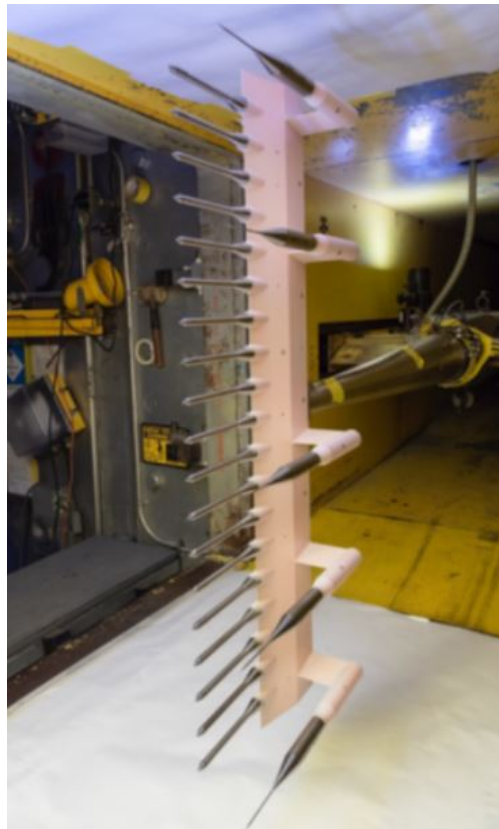


Fig. 1 Flow survey rake (probes numbered 1-19, from top to bottom).

B. Critical Model/Facility Measurements and Instrumentation

Facility and model pressure measurements were primarily obtained using an electronically scanned pressure system (ESP) with digital temperature compensation. ESP modules were tied to a common reference of a hard vacuum (pump maintained vacuum to 5-10 millitorr) so the ESP readings were in absolute pressure units. Different ESP module ranges (5-, 15-, 30-, and 100-psid) were used for different model and facility locations to minimize necessary range (and thus, uncertainty). In-situ ESP calibrations were performed regularly using the system's pressure calibration units to mitigate the effects of thermal drift.

Plenum pressure was measured with a 150-psia range Ruska Series 6000 quartz manometer and plenum total temperature was measured with an Instrulab Platinum RTD, model 4202C. Survey rake temperatures were measured with standard type-K thermocouples referenced to a Kaye Universal Temperature Reference (UTR) RTD.

C. Test Description

A comprehensive description of the UPWT flow survey test is presented in Reference [2]. Testing was conducted with the flow survey rake positioned at different lateral locations within the test section, with YRAKE set points varying out to 12 inches to the left or right of centerline. Data were acquired with the survey rake at a variety of Mach and Reynolds number combinations. Test section Mach numbers ranged from 2.3 to 4.6, and Reynolds numbers ranged from 1 million per foot to 4.5 million per foot.

A run was defined as an axial sweep of the survey rake traversing through a series of XRAKE set points, conducted at a constant Mach and Reynolds number. Data were acquired with the rake probe axial locations varying from XRAKE=0 to 60 inches along the test section. The test section entrance is at XRAKE=0. The measurement center of the test section is located axially at XRAKE=30. This is where most wind tunnel models are positioned for data acquisition. At each flow condition prescribed in the test matrix a block of runs were acquired, consisting of axial sweeps performed with the survey rake at different lateral stations in the test section.

A repeat run was typically acquired at the end of a block setting for a particular flow condition. The vast majority of repeat runs were acquired with the survey rake positioned in the center of the test section at YRAKE=0. There was also a smaller subset of long term repeat data acquired throughout the test. Long term repeats were separated by at least a week or more of testing. This paper will primarily focus on the short term repeatability results.

D. Subset of conditions and variables

With so many variables of interest and conditions involved in this test, it is impossible to display thorough results. To give a sample of results that were produced with the methods that will be described, three of the 48 distinct conditions tested throughout the flow survey are used as a subset of representative results. Set point parameters for each selected condition are listed in Table 1. Similarly, a subset of variables of interest were selected and are described in Table 2.

Condition ID	PT (psfa)	TT (°F)	Mach	Re (10^6 /ft)
6	2280.5	125	2.4	3
24	5418.6	125	3.5	4
36	7420.7	150	4.6	3

Table 1 Condition numbers and associated set point parameters.

Variable of Interest	Units	Description
<i>PTC</i>	psia	Flow survey rake pitot pressure
<i>MC</i>	–	Local Mach number
<i>QC</i>	psfa	Local dynamic pressure

Table 2 Description of variables of interest.

IV. Flow Survey Experimental Uncertainty Quantification

An uncertainty estimate in a measurement or calculated quantity identifies an interval about the quantity within which the true value is likely to fall with a defined probability (typically 95%). An uncertainty interval is a critical component of any stated result since the true value of a quantity is never an absolute known. Experimentalists and CFD modelers must do their best to understand and estimate the potential sources of uncertainty that can creep into their measurement- and computationally-derived results.

The experimental uncertainty was separated into two categories: random and systematic. Random uncertainty was quantified using direct analysis of repeats, a statistical approach using derived values of interest from repeat data acquired. This direct analysis was preferred over random uncertainty propagation techniques to eliminate the risk of improper handling of measurement correlations in the propagation simulation, which can lead to drastic over- or under-estimation of random effects.[3] The term "repeatability" is used interchangeably with random uncertainty. Systematic uncertainty was determined via a first-order Monte Carlo propagation, in which uncertainty was propagated from elemental source estimates and assumed distributions to the derived variables of interest. Systematic and random uncertainty estimates were combined according to their probability distributions to obtain a total uncertainty estimate for variables of interest.

In addition to the purely probabilistic approach described above, a partially probabilistic method was performed via second-order Monte Carlo propagation. Systematic uncertainties formerly treated probabilistically were treated as epistemic uncertainties (with unknown probability distributions).[4] This approach resulted in the development of a family of cumulative distribution functions (CDFs), one CDF for each set of epistemic inputs, reduced to a "probability box" or "p-box" where upper and lower bounding CDF curves define the uncertainty of the variable of interest.

A. Experimental Repeatability

Results were determined from analyzing the repeat data on values of interest. Repeat runs were acquired at virtually every test condition throughout the duration of this test. For each group of repeat runs, the ranges and averages were computed for every set of repeat data points. Repeat runs were typically acquired near the end of a block of runs conducted at the same Mach and Reynolds number.

After the first week of testing, it was discovered that small pieces of tape approximately 0.008 inches in thickness, which had been placed on the rake body and the west test section door as targets for optical measurements, were creating small disturbances and asymmetries in the lateral flow. The targets were subsequently removed for the remainder of the test, and it was therefore decided that the runs influenced by tape targets would be excluded from the repeatability analysis. Within each group of repeat runs, the range (maximum value minus the minimum value) of each measured variable of interest was computed for the repeat data points at every XRAKE set point in the sweep. The ranges were then normalized by the bias correction factor d_2 , which is used to convert range into an estimate of the standard deviation. The value of d_2 is based on the group size, and for group sizes of two $d_2 = 1.128$.

Once all of the repeat run sets were extracted from the test data, normalized ranges were computed for every measured parameter in each group of repeat data points acquired at each XRAKE set point in the run. The ranges were inspected to determine their sensitivity to test section Mach and Reynolds number. There was no significant effect of Reynolds number on the repeatability of any measured variable of interest. Therefore, ranges computed at the same nominal Mach number were pooled together, and the overall estimates of repeatability were computed as a function of Mach. In order to visualize the variation in repeat data in the test section, the average range was computed for each rake probe measurement at each XRAKE set point. This produced a grid of average ranges that cover the vertical test section space from -18 to +18 inches (ZRAKE) and the axial space in the test section (XRAKE) from 0 to 60 inches. Figure 2 shows the averaged normalized ranges of local Mach (MC) measured with the survey rake probes, for the three nominal test Mach numbers listed in Table 1. The x-axis represents the axial position along the length of the test section, the y-axis represents vertical position in the test section, and the contours represent magnitudes of the average normalized range in this plane, based on the 19 local Mach probe measurements acquired at axial test section locations between 0 and 60 inches. The dashed line at XRAKE=30 indicates the axial center of the test section, where the measurement center for most wind tunnel models are located for testing. Note that the color scale is the same for all three plots in Figure 2.

In the core flow region (approximately ten inches above and below the tunnel centerline), the magnitude of the averaged MC ranges increased slightly as nominal Mach number increased. Thus, the random uncertainty of local Mach measurements for nominal test section Mach numbers of 2.4 was slightly less than at nominal Mach numbers of 4.6 (see Table 3. In general, the ranges computed from repeat MC data acquired with probes 5 through 15 (ZRAKE=+10 to -10 inches) were small values. Contour levels equivalent to an average normalized range of 0.001 were highlighted with

white text labels in Figure 2 in order to more easily visualize the slightly different levels of variation in the MC repeat data seen in Figure 2c. Comparing the contour plots for Mach 2.4 (Figure 2a) and Mach 4.6 (Figure 2c), it is evident that the maximum ranges were higher at nominal Mach numbers of 4.6.

While there were not significant axial variations in the random uncertainty for local Mach number probe measurements, there were vertical variations in the uncertainties, particularly at higher nominal Mach numbers. This was observed in the increased magnitude of the averaged ranges of the outer probe data, at the top and bottom of the survey rake, as the outer probes began to be impacted by the boundary layer at the top and bottom of the test section. This effect became more pronounced as the boundary layer thickness increased with the nominal test section Mach number. For Mach 2.4 (Figure 2a there was a narrow region approximately 16 to 18 inches above the tunnel centerline (6 to 8 inches away from the ceiling) with average range values approaching 0.002. As the nominal Mach increased to 3.5 in Figure 2b, this region of higher values became slightly more prominent across the upper test section. At Mach 4.6 (Figure 2c) there were significantly higher levels of variation in repeat measurements along the length of the ceiling and floor, with average range values as high as 0.003, extending several inches into the test section and impacting these outer rake probe measurements.

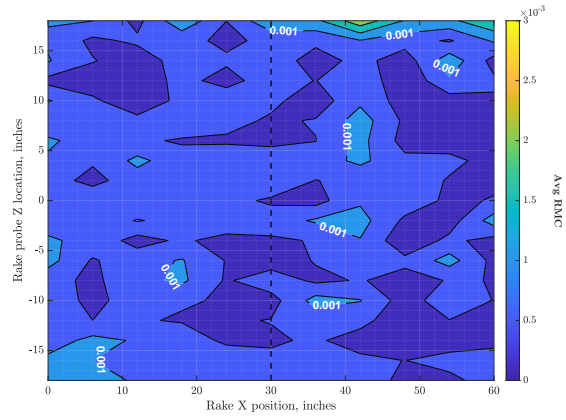
Similar axial and vertical test section trends were seen, to varying degrees, in the repeatability of other measured parameters, as illustrated in Figures 3 and 4, for PTC and QC measurements respectively. These results indicate that there are different levels of random uncertainty in the test section. The uncertainty due to repeatability is highest near the test section ceiling and floor, where the boundary layer affects the measurement quality (rake probes 1-4 and 16-19). Meanwhile the repeatability uncertainty is lowest in the center of the test section (probes 5-15, ZRAKE=+10 to -10 inches) where wind tunnel testing is conducted and model data are measured.

For this particular test, the group size of the applicable short term repeat runs was nearly always two ($n=2$). Consequently, histograms of the theoretical range distribution could be computed and compared with histograms of the actual normalized ranges. If the actual histogram compares favorably to the theoretical histogram, then one can assume the ranges are normally distributed. The theoretical range distribution is converted to a histogram by integrating the theoretical distribution over the same range intervals in the actual distribution [5]. An example is presented in Figure 5 for local Mach probe data at a nominal Mach number of 3.5. The gray bars in Figure 5 represent the normalized ranges for MC measurements for probes 5 through 15. These data compare favorably to the theoretical range distribution represented by the solid red line. The vertical magenta line represents the upper control limit for ranges computed as shown in equation 1, and it covers over 99% of the ranges. These two observations suggest it is reasonable to assume a normal distribution for these pooled ranges. A range histogram plot for MC measurements at probe 10 (RMC10) is also shown in Figure 6. The MC range histogram for a single probe is somewhat coarser, but the trends are similar and the upper limit covers all of the ranges. The overall standard deviation for each measured parameter was computed using the median absolute deviation of the pooled ranges (probes 5-15) for each nominal Mach number, as shown in equations 2 and 3. The two-sigma random uncertainties for the selected parameters of interest are presented in Table 4. Separate standard deviations were also computed for individual probes by applying these equations to the ranges for each probe and nominal Mach number, resulting in an estimate of the random uncertainty for each individual probe variable.

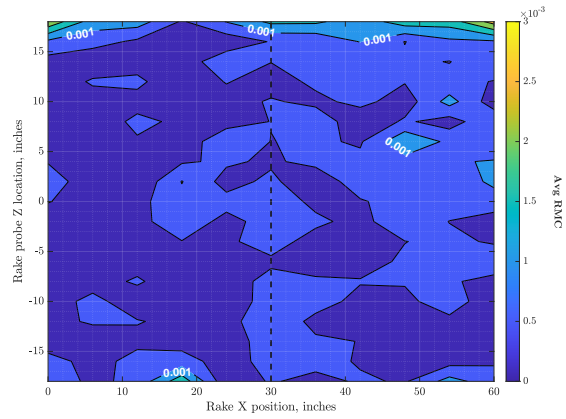
$$UL = 3.864 * \tilde{R} \quad (1)$$

$$MAD = \text{median}(|R - \tilde{R}|) \quad (2)$$

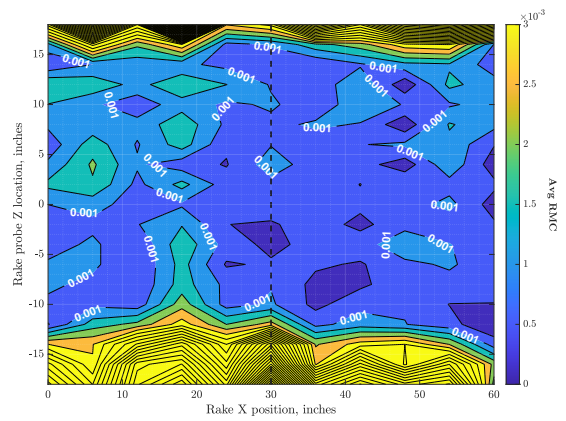
$$\sigma = MAD * 1.4826 \quad (3)$$



(a) Mach=2.4

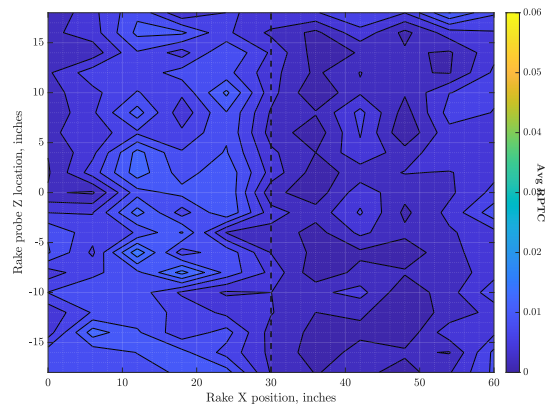


(b) Mach=3.5

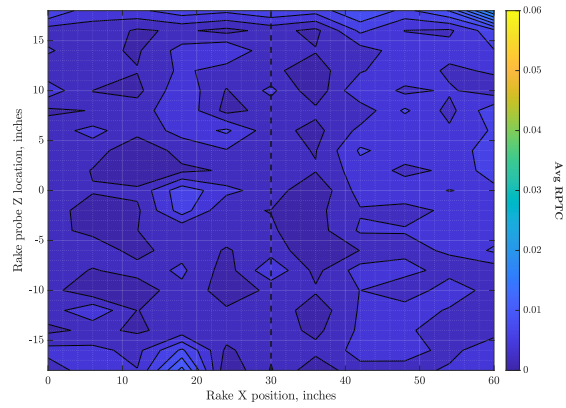


(c) Mach=4.6

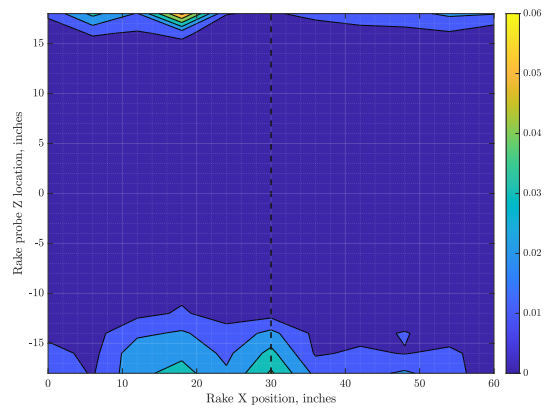
Fig. 2 Contours of averaged ranges of measured probe MC values at YRAKE=0.



(a) Mach=2.4

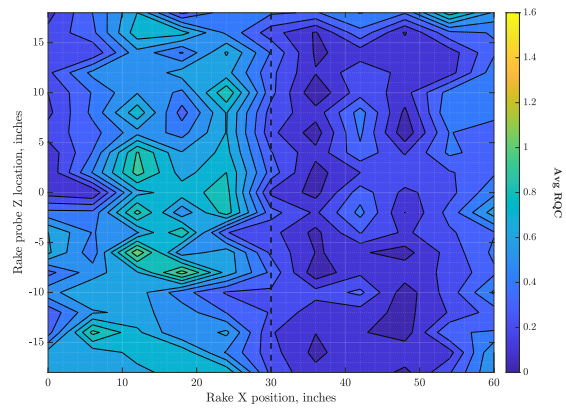


(b) Mach=3.5

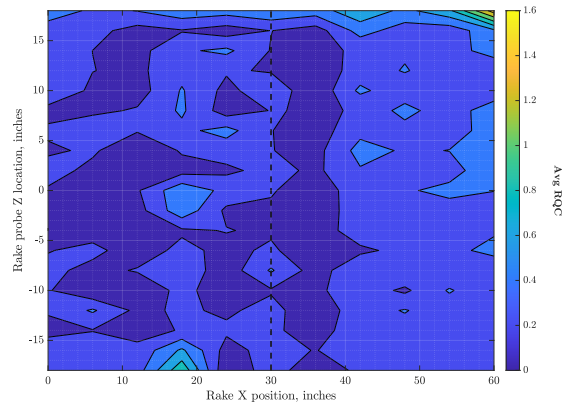


(c) Mach=4.6

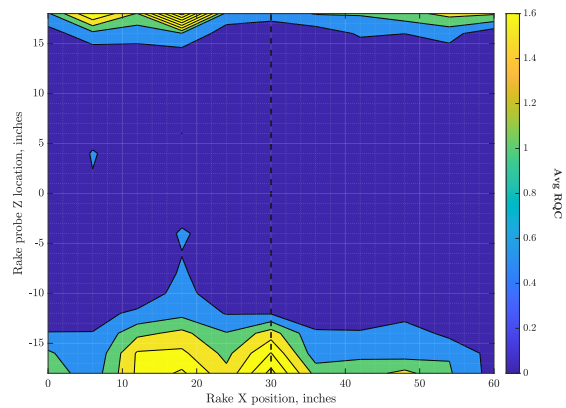
Fig. 3 Contours of averaged ranges of measured probe PTC values at YRAKE=0.



(a) Mach=2.4



(b) Mach=3.5



(c) Mach=4.6

Fig. 4 Contours of averaged ranges of measured probe QC values at YRAKE=0.

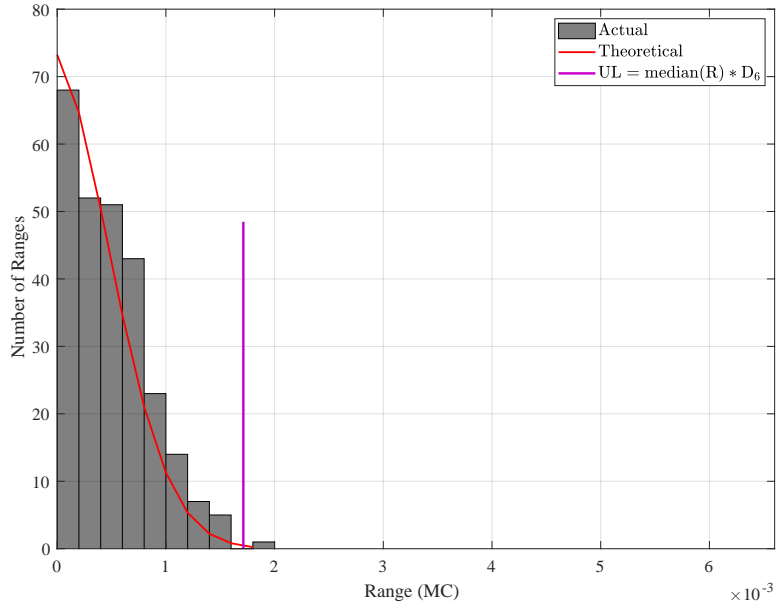


Fig. 5 Theoretical and actual histogram of MC normalized ranges for probes 5-15, Mach 3.5.

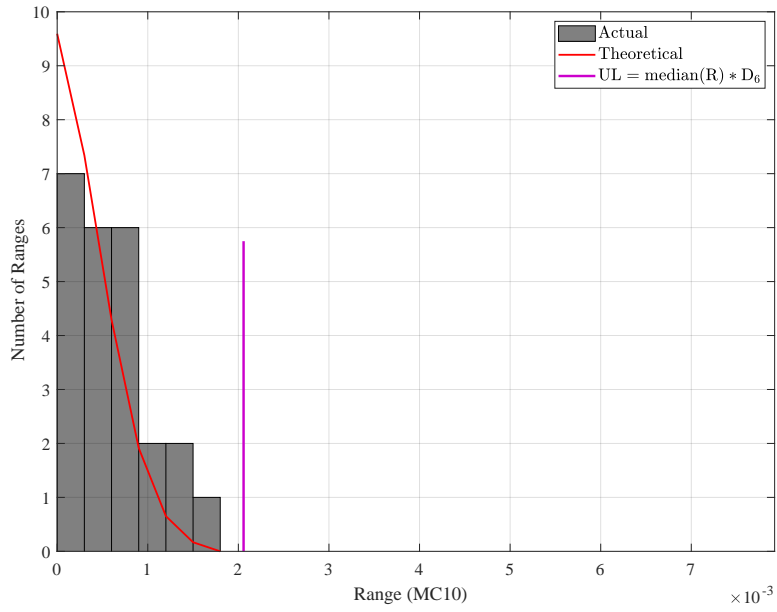


Fig. 6 Theoretical and actual histogram of MC normalized ranges for probe 10, Mach 3.5.

B. Systematic Uncertainty Propagation via Monte Carlo Method

A purely probabilistic approach was used to estimate and propagate systematic uncertainties with assumed error distributions on multiple uncertainty sources using a first-order Monte Carlo uncertainty propagation. Uncertainty sources considered in this analysis were limited to instrumentation system components. Table 3 lists the elemental systematic uncertainty estimates and the error population parameters applied in the Monte Carlo simulation.

Measurement device	Critical measurements	Units	Distribution	Distribution parameters
Ruska Series 6000 Quartz Manometer	Plenum total pressure	psia	Gaussian	$\mu = 0, \sigma$: see Figure 7
Platinum RTD Instrulab 4202C	Plenum total temperature	°R	Gaussian	$\mu = 0, \sigma = 0.135$
Edgetech Dew Master	Facility dew point	°F	Gaussian	$\mu = 0, \sigma = 0.18$
Type K thermocouple	Probe temperature	°F	Gaussian	$\mu = 0, \sigma = 1.98$
Kaye UTR RTD	TC temperature reference	°F	Gaussian	$\mu = 0, \sigma = 0.09$
Druck 15-psia	Tunnel wall pressures	psia	Gaussian	$\mu = 0, \sigma = 0.006$
ESP, 5-psi	Tunnel wall, rake body, static probe and 5-hole cone probe surface pressures	psia	Gaussian	$\mu = 0, \sigma = 0.0025$
ESP, 5-psi PCU	Pressure calibration unit, 5-psi modules	psi	Gaussian	$\mu = 0, \sigma = 0.0005$
ESP, 15-psi	5-hole cone probe and boundary layer probe total pressures	psia	Gaussian	$\mu = 0, \sigma = 0.0075$
ESP, 15-psi PCU	Pressure calibration unit, 15-psi modules	psi	Gaussian	$\mu = 0, \sigma = 0.0015$
ESP, 30-psi	Tunnel wall pressures	psia	Gaussian	$\mu = 0, \sigma = 0.015$
ESP, 30-psi PCU	Pressure calibration unit, 30-psi modules	psi	Gaussian	$\mu = 0, \sigma = 0.003$
ESP, 100-psi	Tunnel wall pressures	psia	Gaussian	$\mu = 0, \sigma = 0.05$
ESP, 100-psi PCU	Pressure calibration unit, 100-psi modules	psi	Gaussian	$\mu = 0, \sigma = 0.01$

Table 3 Elemental systematic uncertainty estimate parameters.

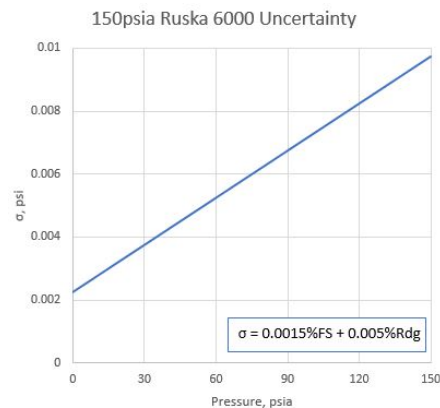


Fig. 7 150-psia Ruska 6000 uncertainty.

Excitation voltages, signal conditioners and analog-to-digital converters used in the measurement systems had negligible uncertainty contributions relative to the instruments listed in Table 3. Each ESP pressure calibration unit (PCU) uncertainty was considered fully correlated among all common-range modules and measurement channels since

simultaneous calibrations were applied. The Kaye UTR thermocouple reference was also considered fully correlated among all thermocouple readings obtained simultaneously at a given test point.

A set of seed data, representing a group of nominal measurement values at wind tunnel conditions of interest, was used in conjunction with the elemental uncertainty estimates to initialize the Monte Carlo simulation. For each measurement in the seed data set, random draws from appropriate random number populations (described by the distributions and parameters in Table 3) were performed for all sources impacting the measurement. This procedure simulated measurement errors, perturbing the set of seed data. The perturbed data were used in the standard facility data reduction scheme to calculate results of interest. This procedure was performed several thousand times until convergence was achieved to produce a large population of results of interest, for which Gaussian distributions resulted and 2-sigma, 95% coverage intervals were defined as the systematic uncertainties of the outcomes. Results from this first-order MC simulation for selected conditions and variables of interest are shown in Table 4.

C. Total Experimental Uncertainty

Figure 8 depicts the two routes of uncertainty estimation for random and systematic components, and the combining of those results to achieve total experimental uncertainty estimates.

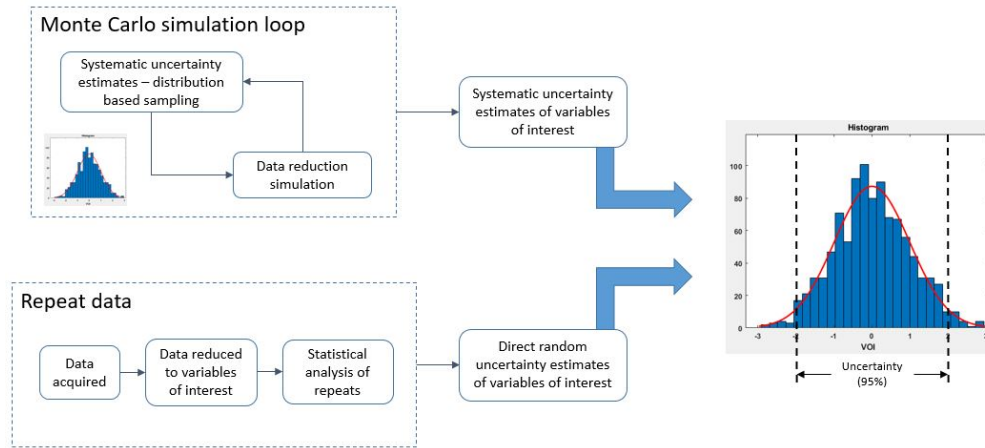


Fig. 8 Purely probabilistic total uncertainty estimation flow chart.

By nature, random uncertainty exhibits a Gaussian distribution. The systematic uncertainty propagation resulted in Gaussian distributions for all variables of interest as well, so combining the two uncertainty components was a very straightforward root-sum-square. An example summary of random, systematic and total uncertainty results for the subset of conditions and variables of interest are shown in Table 4.

Condition ID	Variable of Interest	Nominal Value	2- σ Systematic Uncertainty	2- σ Random Uncertainty	2- σ Total Uncertainty
6	MC	2.40	0.0023	0.00079	0.0025
24	MC	3.50	0.0023	0.00079	0.0024
36	MC	4.60	0.0045	0.00156	0.0048
6	PTC	8.53 psia	0.015 psi	0.0083 psi	0.017 psi
24	PTC	7.88 psia	0.015 psi	0.0049 psi	0.016 psi
36	PTC	4.29 psia	0.015 psi	0.0053 psi	0.016 psi
6	QC	627.3 psfa	1.05 psf	0.589 psf	1.206 psf
24	QC	600.0 psfa	1.15 psf	0.369 psf	1.203 psf
36	QC	330.5 psfa	1.19 psf	0.395 psf	1.251 psf

Table 4 Total uncertainty results for variables of interest in UPWT test section.

1. Second-order Monte Carlo Analysis

A purely probabilistic approach such as the first-order Monte Carlo can be useful for making simple uncertainty assessments, but there is risk in doing so. Many uncertainty estimates that are not well-defined require assumptions about the error distributions they represent in order to perform the first-order uncertainty propagation method. Instrument manufacturers provide specifications that include accuracy levels, but there is a general lack of standards in how those uncertainty levels are defined and quoted. Some manufacturers provide a single accuracy value while some provide detailed source breakdowns. Rarely are error distributions or interpretations of accuracy stated in a specification document, making assumptions inevitable. Assumptions of distributions can produce misleading results in a fully probabilistic approach, as described in Walker, et.al.[4]

Alternatively, a mixed uncertainty model can be created in which uncertainties formerly treated as systematic are treated as epistemic, or uncertainty arising from lack of knowledge (such as unknown distributions of uncertainty sources).[6] Instead of making assumptions about the distributions and treating the uncertainties purely probabilistically, an interval bounding each uncertainty source can be defined. A nested-loop Monte Carlo propagation can be used which samples these epistemic uncertainty sources via Latin hypercube sampling (LHS) in the outer loop before performing a high-iteration inner loop where the random uncertainty is applied. The result of each outer loop iteration is a CDF representing the set of outcomes of variables of interest from the inner loop propagation. Performing the outer loop many times over produces a family of CDFs, the upper and lower bounds of which can be used to form a p-box, a useful tool in uncertainty quantification and risk assessment. A flow chart of this method is depicted in Figure 9.

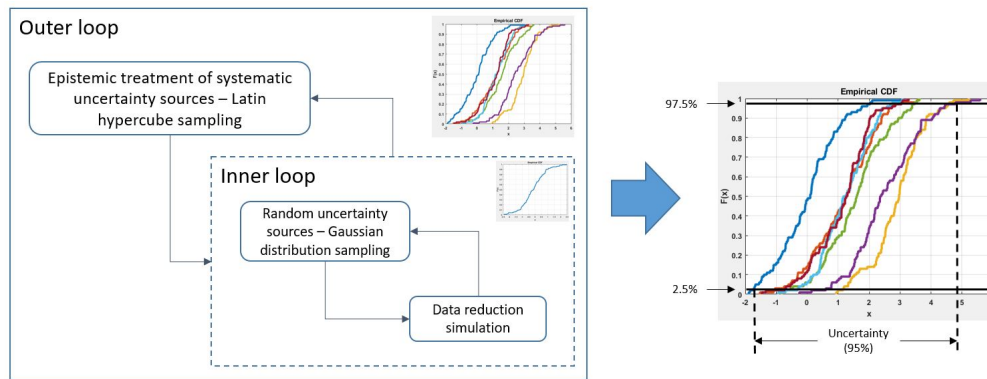


Fig. 9 Partially probabilistic total uncertainty estimation flow chart[4]

This second-order Monte Carlo propagation was used on the UPWT Flow Survey data to supplement the information provided by the first-order analysis. With both types of results available, those performing CFD comparisons can select which treatment of the systematic uncertainty sources best fit the scope of the comparison being made. Computation time was not a limitation for this straightforward data reduction scheme, so 500 outer loop iterations were run nested with several thousand inner-loop iterations. P-box results for Conditions 6, 24 and 36 for *PTC*, *MC*, and *QC* are shown in Figure 10.

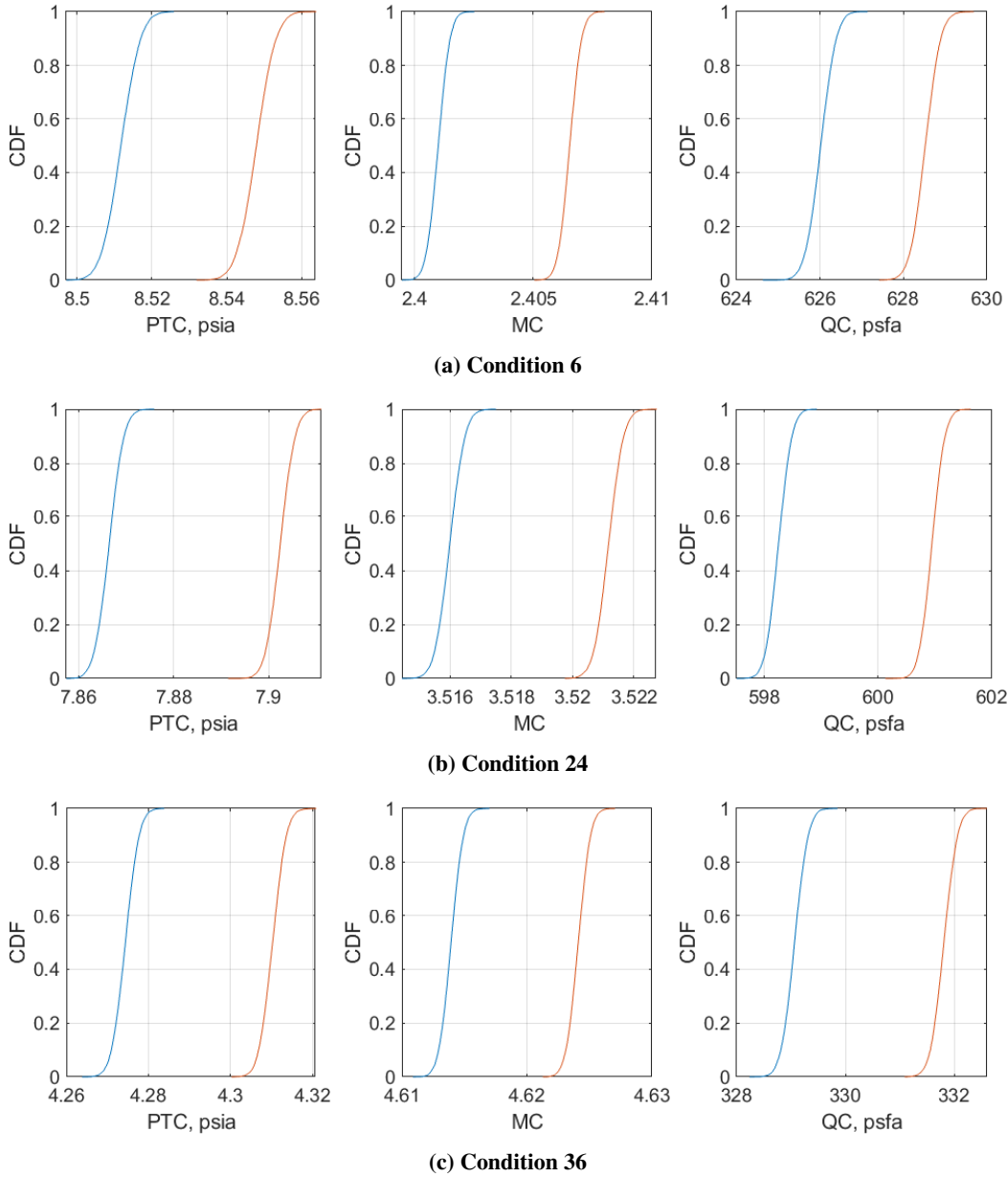


Fig. 10 Probability boxes for selected conditions and variables of interest.

V. Comparison of CFD and Flow Survey Experimental Results

As it pertains to this CFD comparison study, ideally both the experimentally derived value's uncertainty bounds and CFD outcome's uncertainty overlap one another and mutually contain the true value of interest. To date, computational flow predictions have been run using the CFD codes FUN3D, Overflow, and USM3D. Predictions were also obtained using FUN3D with an adaptive grid.[7] The uncertainty quantification for the CFD results was not yet finalized at the writing of this paper. However, comparison plots of CFD and wind tunnel data with corresponding 2-sigma estimated experimental uncertainty bars are presented in Figures 11 and 12 for flow conditions 24 and 36, respectively. In these plots, the black circles represent wind tunnel data, and the various colored solid lines represent CFD results obtained with different flow solvers. All data are presented at the test section center ($X=30$ in., $Y=0$ in.). The horizontal error bars accompanying the wind tunnel data points represent the total 2-sigma uncertainties computed as described in this paper and summarized in Table 4. At condition 24 (Mach 3.5) shown in Figure 11), the FUN3D with adaptive grid and

USM3D predictions for pitot pressures (PTC) at test section heights from -10 to +10 inches tended to compare most favorably to the wind tunnel data. All four CFD results for Mach (MC) were very similar to one another in this same region. Towards the top and bottom of the survey rake, there are greater differences between CFD predictions where the flow around the rake begins to be impacted by the test section boundary layer. The wind tunnel data for probes 7 and 8 appeared to diverge from the trends in the rest of the survey rake measurements at this Mach number. This was likely due to some non-uniformity, of unknown origin, in the flow in the $Y=0$ plane. The non-uniformity disappears as one moves away laterally from the $Y=0$ plane. The Mach and pressure profiles for condition 36 (Mach 4.6), shown in Figure 12, were quite different from those at Mach 3.5. There appears to be slightly more scatter between the various CFD predictions, which also coincides with the larger experimental uncertainties computed for this Mach number. This might suggest that this flow condition is more complex or challenging to model. Note that three Overflow solutions were run at this condition, each with different grid fineness and turbulence model settings. At this flow condition, the solver Overflow ('OVERFLOW 015') appeared to compare the closest to experiment.

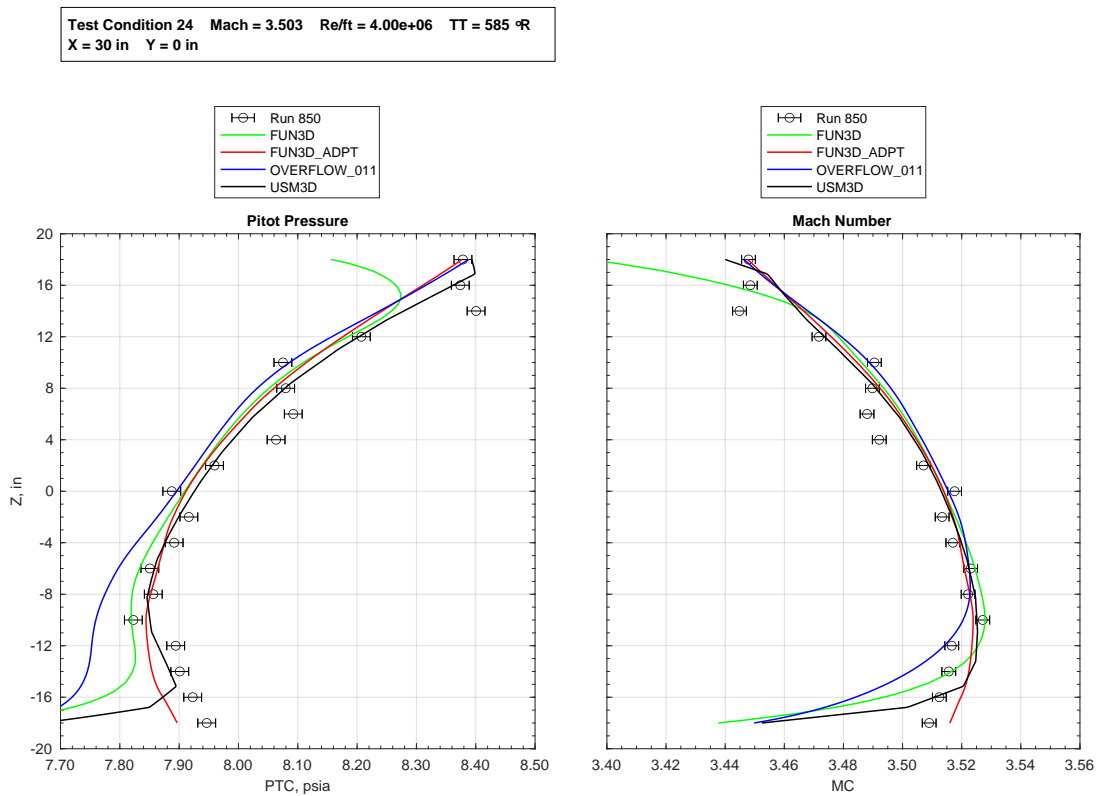


Fig. 11 Comparison of experimental and CFD local pressure and Mach profiles for condition 24 at X=30 and Y=0.

Test Condition 36 Mach = 4.631 Re/ft = 3.00e+06 TT = 610 °R
 X = 30 in Y = 0 in

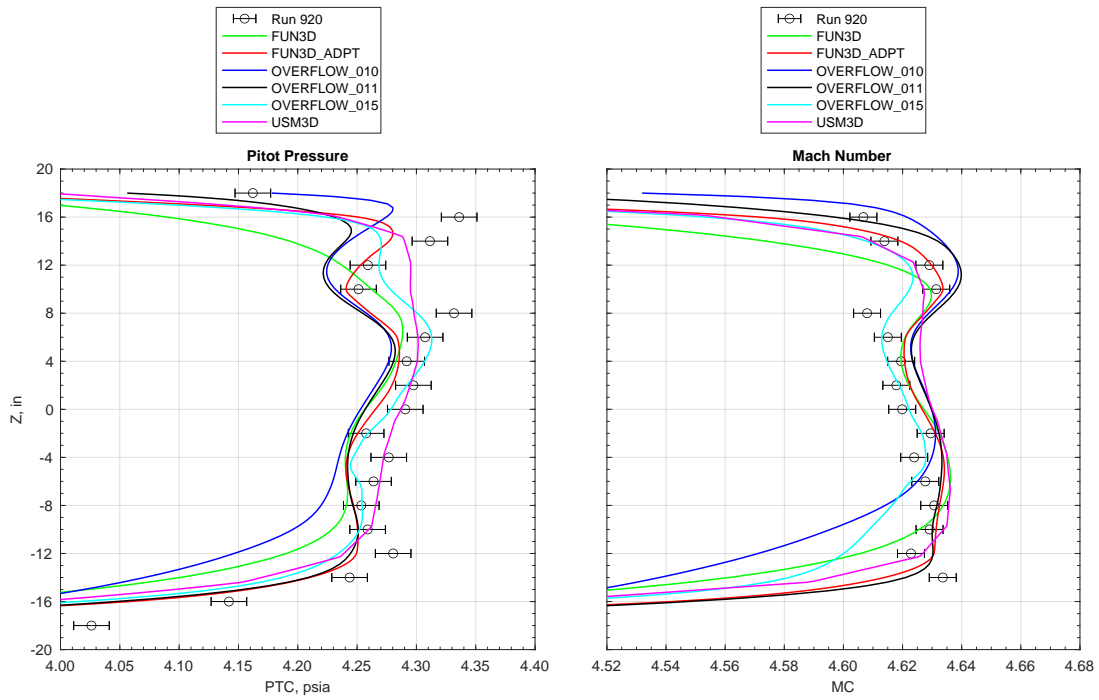


Fig. 12 Comparison of experimental and CFD local pressure and Mach profiles for condition 36 at X=30 and Y=0.

VI. Conclusion

The primary purpose of this paper was to provide documentation of the experimental uncertainty quantification approach for the UPWT Flow Survey test. Random and systematic uncertainty quantification methods were described and results were shown for a subset of the test conditions and variables of interest. Random uncertainty was evaluated directly from repeat data acquired for several variables of interest. Systematic uncertainty was determined via propagation using two distinct treatments of instrumentation-based measurement uncertainty for future flexibility in experiment-to-CFD comparisons. Several other conference papers from the “Evaluation of CFD as a Surrogate for Wind-Tunnel Testing” series used the results from this analysis for experimental data comparisons to UPWT empty tunnel CFD. It is expected that the remaining tests in this series will use a similar approach to experimental uncertainty quantification, though additional sources of uncertainty such as tunnel calibration, flow angle corrections, and force-balance corrections will be applied along with instrumentation-based measurement uncertainty.

Acknowledgments

The authors wish to acknowledge and thank Matt Rhode for supplying the images in Figures 11 and 12.

References

- [1] Charlie M. Jackson, W. A. C., Jr., “Description and Calibration of the Langley Unitary Plan Wind Tunnel,” Tech. rep., NASA TP-1905, 1981.
- [2] Rhode, M. N., et al., “Flow Characterization of the NASA Langley Unitary Plan Wind Tunnel, Test Section 2: Experimental Results,” Conference Paper TBD, American Institute of Aeronautics and Astronautics, Virtual, 2-6 August 2021.
- [3] Coleman, H. W., and Steele, W. G., *Experimentation, Validation and Uncertainty Analysis for Engineers*, Third ed., John Wiley and Sons, Inc., 2009.
- [4] Walker, E. L., et al., “Integrated Uncertainty Quantification for Risk and Resource Management: Building Confidence in Design (Invited),” Conference Paper AIAA 2015-0501, American Institute of Aeronautics and Astronautics, Kissimmee, FL, 5-9 January 2015.
- [5] Hemsch, M. J., “Statistical Analysis of SLS Aero-Acoustic CFD-to-WT Comparisons,” , 7 December 2016. NASA Langley Space Launch System Aero Team Memo.
- [6] Eldred, M. S., and Swiler, L. P., “Efficient Algorithms for Mixed Aleatory-Epistemic Uncertainty Quantification with Application to Radiation-Hardened Electronics, Part 1,” Report SAND2009-5805, Sandia National Laboratories, September 2009.
- [7] Childs, R., et al., “Flow Characterization of the NASA Langley Unitary Plan Wind Tunnel, Test Section 2: Computational Results,” Conference Paper TBD, American Institute of Aeronautics and Astronautics, Virtual, 2-6 August 2021.